Deep level defects in a nitrogen-implanted ZnO homogeneous *p-n* junction

Q. L. Gu,[1] C. C. Ling,[1,a)] G. Brauer,[2] W. Anwand,[2] W. Skorupa,[2] Y. F. Hsu,[1] A. B. Djurišić,[1] C. Y. Zhu,[1] S. Fung,[1] and L. W. Lu[1]
[1]*Department of Physics, The University of Hong Kong, Pokfulam Road, Hong Kong, People's Republic of China*
[2]*Institut für Ionenstrahlphysik und Materialforschung, Forschungszentrum Dresden-Rossendorf, Postfach 510119, D-01314 Dresden, Germany*

(Received 15 January 2008; accepted 13 May 2008; published online 5 June 2008)

Nitrogen ions were implanted into undoped melt grown ZnO single crystals. A light-emitting *p-n* junction was subsequently formed by postimplantation annealing in air. Deep level transient spectroscopy was used to investigate deep level defects induced by N^+ implantation and the effect of air annealing. The N^+ implantation enhanced the electron trap at $E_C-(0.31\pm0.01)$ eV (E3) and introduced another one at $E_C-(0.95\pm0.02)$ eV (D1), which were removed after annealing at 900 and 750 °C, respectively. Another trap D2 ($E_a=0.17\pm0.01$ eV) was formed after the 750 °C annealing and persisted at 1200 °C. © *2008 American Institute of Physics*. [DOI: 10.1063/1.2940204]

ZnO has recently received attention because of its applications in optoelectronics and spintronics.[1,2] Undoped ZnO is of *n* type. Asymmetry difficulty in *p*-type doping of ZnO is a major obstacle for device applications, although progress has recently been made with N, As, P doping, and codoping with group III and V elements.[2] Ion implantation is useful for a selective region doping, but it inevitably introduces undesirable defect. This is particularly important for ZnO as the compensating intrinsic donors have low formation energy and are energetically stable.[3,4] There have been only a few reports of *p*-ZnO induced by ion implantation [N^+ (Refs. 5–8) and As^+ implantations (Ref. 9)] and the ion-implantation induced defects were poorly understood. Because of difficulties in making a junction, deep level transient spectroscopy (DLTS) studies have also been very few.[8,10–16]

In this study, N^+ ions were implanted into the *n*-type melt grown (MG) ZnO single crystal and no rectifying property was observed in the as-implanted sample. A homogeneous *p-n* junction which emitted light at room temperature (RT) was formed after the postimplantation annealing. Deep level defects in the structure and also their thermal evolution were studied by DLTS.

The starting material was one-side polished undoped *n*-type MG ZnO (0001) substrate ($n=5\times10^{16}$ cm^{-3} and $\mu=203$ cm^2 V^{-1} s^{-1}) from Cermet Inc. N^+ ions were implanted into the polished front side (F-side) at 300 °C with energy of 150 keV (fluence of 10^{14} cm^{-2}). This corresponds to a N-implantation profile peaking at ~270 nm (calculated by the program TRIM (Ref. 17) and measured by secondary-ion-mass spectroscopy). Ohmic contacts were fabricated by evaporating 50 nm Al film onto the samples. The postimplantation annealing was performed in air for 30 min. *C-V*, *I-V*, and DLTS measurements were made using a HP4155A semiconductor parameter analyzer and a Sula Technologies DLTS system, respectively. The DLTS measurements employed a reverse bias and a filling pulse voltage of $V_R=-2$ V and $V_P=0$ V. The activation energy E_a, capture cross section σ, and concentration N_T of the traps were calculated by the Arrhenius plot.[18] To fabricate a light-emitting diode (LED) for electroluminescence (EL) measurement, four-folded N^+ implantations with energies of 80, 180, 310, and 500 keV (with fluences of ~10^{14} cm^{-2}) were carried out on the same raw ZnO sample. This resulted in a ~1 μm deep box-shaped region with N concentration ~6×10^{18} cm^{-3}. Then a 750 °C air annealing was performed. A ~50 nm thick ITO film was evaporated on the implanted side using an electron beam evaporator while keeping the sample at 250 °C.[19] The EL spectra were collected using a monochromator (Acton SpectraPro 500i) and a Peltier-cooled photomultiplier detector (Hamamatsu R636-10).

I-V data in Fig. 1 showed that the as-implanted sample has no rectifying property. However, rectifying behavior was observed for samples annealed at 650, 750, 900, and 1200 °C in air, which indicated the formation of *p* layer in the N^+-implanting region. Their leakage currents at −1.5 V were 1270, 43, 12, and 140 nA, respectively. Referring to the *C-V* measurement scheme in Ref. 20 the hole concentrations of the *p*-type layers were estimated to be ~10^{17} cm^{-3}. The thermoelectric probe measurements performed on the annealed N^+-implanted samples also confirmed the *p*-layer formation.

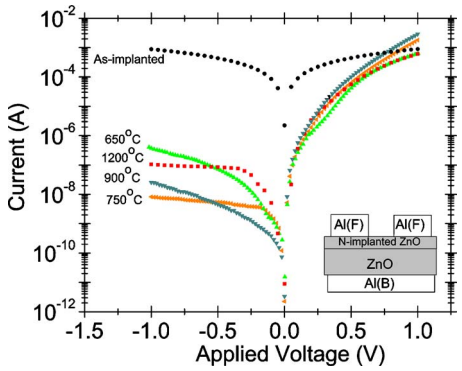

FIG. 1. (Color online) *I-V* data of the N^+-implanted undoped MG ZnO samples with different postimplantation annealing temperatures in air. The *I-V* measurements were performed across the Al(F)-Al(B) connection.

a)Author to whom correspondence should be addressed. Electronic mail: ccling@hku.hk.

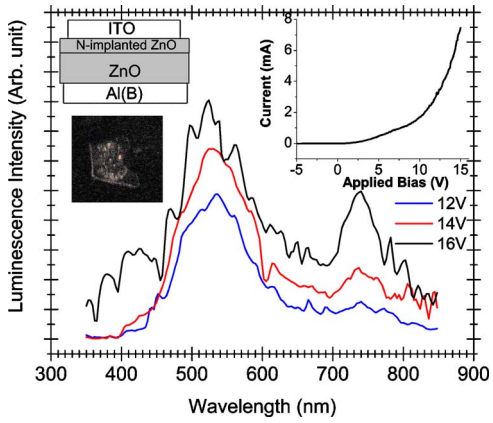

FIG. 2. (Color online) EL spectra of the N-implanted ZnO homogeneous *p-n* junction taken at RT. The *IV* character of the *p-n* junction is shown in the inset at the top right corner. The device schematic diagram and the LED photo are shown at the top left corner.

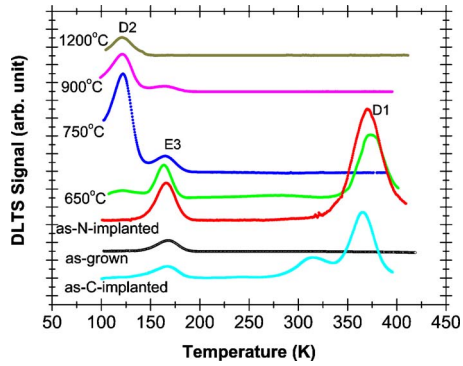

FIG. 3. (Color online) DLTS spectra of the N^+-implanted undoped MG ZnO samples annealed at different temperatures. The DLTS spectra of the as-grown ZnO and the as-C^+-implanted ZnO samples are included for reference. The measurements were taken with the rate window, the reverse bias voltage, the filling pulse width, and the filling pulse voltage equal to $\Delta t = 21.5$ ms, $V_R = -2$ V, $t_P = 1$ ms, $V_P = 0$ V.

The RT EL spectra of the forward biased LED (Fig. 2) shows two broad peaks at ~530 nm (~2.34 eV) and ~740 nm (~1.68 eV). Their peak intensities increase with forward bias voltage. The observed light emission clearly demonstrated the formation of a *p-n* junction in the annealed N-implanted ZnO samples.

To carry out DLTS study on the nonrectifying as-implanted and nonimplanted samples, Au rectifying contacts were fabricated on the F-side of the samples pretreated with H_2O_2.[21] For the as-grown sample DLTS spectrum, a majority peak (i.e., e^- trap) with $E_a = 0.31$ eV, $\sigma_n \sim 10^{-16}$ cm^{-2}, and $N_T \sim 10^{15}$ cm^{-3} [usually referred to E3 (Refs. 8 and 10–16)] and another one ($E_a = 0.10$ eV, $\sigma_n \sim 10^{-17}$ cm^{-2}, and $N_T \sim 10^{13}$ cm^{-3}) with a much weaker intensity (less than 20 times of E3) were identified. The E3 intensity dropped with annealing temperature, but persisted at 1200 °C annealing. The $E_a = 0.10$ eV level anneals at 900 °C. The DLTS spectrum of the as-N^+-implanted sample is shown in Fig. 3 (the as-grown sample spectrum also included for reference), which shows that N implantation enhances the E3 intensity and introduces another e^- trap at ~360 K (D1) having $E_a = 0.94$ eV and $\sigma_n \sim 10^{-14}$ cm^{-2}.

Figure 3 shows the DLTS spectra of the annealed N^+-implanted *p-n* junctions. Biasing at $V_R = -2$ V during the DLTS measurements corresponded to a depletion of ~30 and 100 nm extending to the *p* and *n* sides, respectively. It is thus difficult to determine the nature (i.e., e^- trap or h^+ trap) of the signals identified in these spectra. However, the two majority peaks at ~160 and 360 K in these annealed sample spectra have E_a and σ_n (as shown in Table I) agreeing well to the E3 and D1 already identified in the as-grown and the as-implanted samples, and are thus attributed to E3 and D1. The E3 concentration decreases with annealing temperature and reduces by a factor of ~100 after the 900 °C annealing. D1 annealed out at 750 °C. Referring to Fig. 3, another majority peak (D2) at ~120 K with $E_a = 0.17$ eV and $\sigma_n \sim 10^{-16}$ cm^{-2} was introduced after 750 °C annealing. However, it is not certain as to whether this is an e^- or a h^+ trap. Its concentration drops with annealing temperature, but persists at 1200 °C.

Although DLTS itself cannot offer definitive information about the defect microstructure, it would still be useful to explore the possible origins of the identified defects E3, D1, and D2. E3 is commonly observed in as-grown ZnO single crystals.[10] However, its exact microstructure is still controversial and has been attributed to V_O and V_{Zn}-related defects.[10–12,16] In the N^+-implanted sample (Fig. 3), E3 became undetectable upon 1200 °C annealing. However, in the nonimplanted sample, E3 persisted (concentration ~10^{15} cm^{-3}) upon 1200 °C annealing. Thus, the mechanism of the E3 annealing process in the N^+-implanted sample probably involves another defect created by the N^+ implantation.

DLTS measurements were performed also at the Au Schottky contacts fabricated on the as-C^+-implanted and the as-As^+-implanted samples (fluence = 10^{14} cm^{-2} each) using

TABLE I. Activation energies E_a, trap concentrations N_T, and capture cross sections σ_T of the deep level defects introduced by the N implantation.

	Unimplanted	As implanted	650 °C	750 °C	900 °C	1200 °C
E3	$E_a = 0.31$ eV, $N_T \sim 10^{15}$ cm^{-3}, $\sigma \sim 10^{-16}$ cm^2	$E_a = 0.31$ eV, $N_T \sim 10^{16}$ cm^{-3}, $\sigma \sim 10^{-15}$ cm^2	$E_a = 0.32$ eV, $N_T \sim 10^{16}$ cm^{-3}, $\sigma \sim 10^{-15}$ cm^2	$E_a = 0.31$ eV, $N_T \sim 10^{15}$ cm^{-3}, $\sigma \sim 10^{15}$ cm^2	$E_a = 0.31$ eV, $N_T \sim 10^{14}$ cm^{-3}, $\sigma \sim 10^{15}$ cm^2	Annealed out
D1	⋯	$E_a = 0.94$ eV, $N_T \sim 10^{16}$ cm^{-3}, $\sigma \sim 10^{-14}$ cm^2	$E_a = 0.98$ eV, $N_T \sim 10^{16}$ cm^{-3}, $\sigma \sim 10^{-14}$ cm^2	Annealed out	⋯	⋯
D2	⋯	⋯	$E_a = 0.18$ eV, $N_T \sim 10^{15}$ cm^{-3}, $\sigma \sim 10^{-16}$ cm^2	$E_a = 0.17$ eV, $N_T \sim 10^{16}$ cm^{-3}, $\sigma \sim 10^{-16}$ cm^2	$E_a = 0.17$ eV, $N_T \sim 10^{16}$ cm^{-3}, $\sigma \sim 10^{-16}$ cm^2	$E_a = 0.17$ eV, $N_T \sim 10^{15}$ cm^{-3}, $\sigma \sim 10^{16}$ cm^2

the same raw materials. D1 is also observed in the as-C^+-implanted and the as-As^+-implanted samples (the former shown in Fig. 3), hence indicative of being an intrinsic defect. D1's intensity and peak position dependences on t_p (10^{-6}–0.1 s) were also studied while fixing Δt=43 ms. The D1 intensity increases with t_p and saturates at t_p =0.01 s. Its peak position is independent of t_p, which implies D1 is a point defect. D1 is close to the calculated energy state $\varepsilon(2+/0)$ of V_O at E_C−1.0 eV, which possesses negative U behavior.[22] This theoretical result also allowed a detailed and consistent interpretation of the optically detected electron paramagnetic resonance data.[23] We thus tentatively attribute D1 to the $\varepsilon(2+/0)$ state of V_O.

D2 was only formed in the N^+-implanted samples after 750 °C annealing but not in the nonimplanted sample. The formation process of D2 in the N^+-implanted samples thus probably involves other defects created by the implantation. D2 has E_a close to that of a hole trap located at E_V =0.15–0.16 eV identified in particle irradiated ZnO materials.[8,15,24,25] However, further effort is needed to clarify the defect identity.

In conclusion, a ZnO homogeneous p-n junction was formed by N implantation followed by postimplantation air annealing. DLTS study showed that the N^+ implantation enhanced the E3 (E_C=0.31 eV) intensity and induced the level D1 (E_C=0.95 eV), which were removed after 900 and 750 °C annealing, respectively. Another trap D2 (E_a=0.17 eV) was formed after the 750 °C post-N^+-implantation annealing and it persisted after the 1200 °C annealing.

This work was supported by the RGC, HKSAR (7037/06P and G_HK026/07), and the UDG, HKU. The authors thank Professor K. W. Cheah (Hong Kong Baptist University) for the EL measurements.

[1] Ü. Özgür, Ya. I. Alivov, C. Liu, A. Teke, M. A. Reshchikov, S. Doğan, V. Avrutin, S.-J. Cho, and H. Morkoç, J. Appl. Phys. **98**, 041301 (2005).
[2] *Zinc Oxide Bulk, Thin Films and Nanostructures Processing, Properties and Applications*, edited by C. Jagadish and S. J. Pearton (Elsevier, New York, 2006).
[3] S. B. Zhang, S. H. Wei, and A. Zunger, Phys. Rev. B **63**, 075205 (2001).
[4] A. F. Kohan, G. Ceder, D. Morgan, and C. G. Van de Walle, Phys. Rev. B **61**, 15019 (2000).
[5] A. N. Georgobiani, A. N. Gruzintsev, V. T. Volkov, M. O. Vorobiev, V. I. Demin, and V. A. Dravin, Nucl. Instrum. Methods Phys. Res. A **514**, 117 (2003).
[6] C. C. Lin, S. Y. Chen, S. Y. Cheng, and H. Y. Lee, Appl. Phys. Lett. **84**, 5040 (2004).
[7] H. T. Wang, B. S. Kang, J. J. Chen, T. Anderson, S. Jang, F. Ren, H. S. Kim, Y. J. Li, D. P. Norton, and S. J. Pearton, Appl. Phys. Lett. **88**, 102107 (2006).
[8] H. von Wenckstern, R. Pickenhain, H. Schmidt, M. Brandt, G. Biehne, M. Grundmann, and G. Brauer, Appl. Phys. Lett. **89**, 092122 (2006).
[9] G. Braunstein, A. Muraviev, H. Saxena, N. Dhere, V. Richter, and R. Kalish, Appl. Phys. Lett. **87**, 192103 (2005).
[10] J. C. Simpson and J. F. Cordaro, J. Appl. Phys. **63**, 1781 (1988).
[11] F. D. Auret, S. A. Goodman, M. Hayes, M. J. Legodi, H. A. van Laarhoven, and D. C. Look, Appl. Phys. Lett. **79**, 3074 (2001).
[12] F. D. Auret, J. M. Nel, M. Hayes, L. Wu, W. Wesch, and E. Wendler, Superlattices Microstruct. **39**, 17 (2006).
[13] F. D. Auret, S. A. Goodman, M. J. Legodi, W. E. Meyer, and D. C. Look, Appl. Phys. Lett. **80**, 1340 (2002).
[14] M. Hayes, F. D. Auret, P. J. Janse van Rensburg, J. M. Nel, W. Wesch, and E. Wendler, Phys. Status Solidi B **244**, 1544 (2007).
[15] A. Y. Polyakov, N. B. Smirnov, A. V. Govorkov, E. A. Kozhukhova, V. I. Vdovin, K. Ip, M. E. Overberg, Y. W. Heo, D. P. Norton, S. J. Pearton, J. M. Zavada, and V. A. Dravin, J. Appl. Phys. **94**, 2895 (2003).
[16] T. Frank, G. Pensl, R. Tena-Zaera, J. Zúñiga-Pérez, C. Martínez-Tomás, V. Muñoz-Sanjosé, T. Ohshima, H. Itoh, D. Hofmann, D. Pfisterer, J. Sann, and B. Meyer, Appl. Phys. A: Mater. Sci. Process. **88**, 141 (2007).
[17] J. F. Ziegler, J. P. Biersack, and U. Littmark, *The Stopping and Range of Ions in Solids* (Pergamon, New York, 1985).
[18] D. V. Lang, J. Appl. Phys. **45**, 3023 (1974).
[19] R. X. Wang, C. D. Beling, S. Fung, A. B. Djurišić, C. C. Ling, and S. Li, J. Appl. Phys. **97**, 033504 (2005).
[20] C. van Opdorp, Solid-State Electron. **11**, 397 (1968).
[21] Q. L. Gu, C. C. Ling, X. D. Chen, C. K. Cheng, A. M. C. Ng, C. D. Beling, S. Fung, A. B. Djurišić, L. W. Lu, G. Brauer, and H. C. Ong, Appl. Phys. Lett. **90**, 122101 (2007).
[22] A. Janotti and C. G. Van de Walle, Appl. Phys. Lett. **87**, 122102 (2005).
[23] L. S. Vlasenko and G. D. Watkins, Phys. Rev. B **71**, 125210 (2005).
[24] Z. Q. Fang, B. Claflin, D. C. Look, and G. C. Farlow, J. Appl. Phys. **101**, 086106 (2007).
[25] K. Kuriyama, M. Ooi, K. Matsumoto, and K. Kushida, Appl. Phys. Lett. **89**, 242113 (2006).